HAL
open science

Quasi-phase-matched third harmonic generation in optical fibers using refractive-index gratings

Karol Tarnowski, Bertrand Kibler, Christophe Finot, W. Urbanczyk

To cite this version:

Karol Tarnowski, Bertrand Kibler, Christophe Finot, W. Urbanczyk. Quasi-phase-matched third harmonic generation in optical fibers using refractive-index gratings. IEEE Journal of Quantum Electronics, 2011, 47 (5), pp.622-629. 10.1109/JQE.2011.2107888 . hal-00561134

HAL Id: hal-00561134

https://hal.science/hal-00561134v1

Submitted on 31 Jan 2011

HAL is a multi-disciplinary open access archive for the deposit and dissemination of scientific research documents, whether they are published or not. The documents may come from teaching and research institutions in France or abroad, or from public or private research centers.

L'archive ouverte pluridisciplinaire **HAL**, est destinée au dépôt et à la diffusion de documents scientifiques de niveau recherche, publiés ou non, émanant des établissements d'enseignement et de recherche français ou étrangers, des laboratoires publics ou privés.

Quasi-phase-matched third harmonic generation in optical fibers using refractive-index gratings

Karol Tarnowski, Bertrand Kibler, Christophe Finot, Waclaw Urbanczyk

***Abstract*—The purpose of this work is to demonstrate the quasi-phase-matching of third harmonic generation process in optical fibers using refractive-index gratings. We compare conversion efficiency calculated with analytical coupled modes theory and numerical approach employing system of coupled generalized nonlinear Schrödinger equation. Moreover, we show that introducing the phase matching condition that takes into account the nonlinear contribution to propagation constants significantly increases the conversion efficiency by several orders of magnitude. Finally we optimize the grating constant to maximize conversion efficiency.**

***Index Terms*—frequency conversion, gratings, optical fibers, optical phase matching, third harmonic generation**

I. Introduction

In last years, an increasing interest in third harmonic generation (THG) in optical fibers is observed. The first experimental evidence of third harmonic generation in optical fiber dates from 1983 [1]. This observation in elliptical core fiber reported the generation of the third harmonic line of pump and other spectral lines resulting from three-wave sum frequency process. The later investigations showed the correlation between the presence of various dopants in optical fibers, such as germanium, erbium or nitrogen, and third harmonic growth [2]-[4]. In these works, THG efficiencies of about 10^{-5} were obtained. More recently, several studies confirmed the possibility of THG in photonic crystal fibers (PCF) employing intermodal phase matching condition, which greatly enhances the conversion efficiency [5]-[7]. The possibility of phase-matched THG was only demonstrated between the fundamental mode of pump and the higher order modes of TH. Unfortunately, due to high chromatic dispersion, it is impossible to achieve the phase matching condition between the fundamental modes of pump and its third harmonic in conventional optical fibers and highly nonlinear fibers [5],[8]-[10]. Even in photonic crystal fibers, in which the waveguide dispersion can be tailored in a very high degree, it is difficult to fully compensate for the material dispersion of the glass between the pump and its third harmonic [11].

In this work, we propose a concept of overcoming the difficulties in direct phase matching of the pump and its third harmonic by applying the quasi-phase matching (QPM) technique based on refractive index grating written into the fiber. The QPM concept was first proposed in 1962 by Armstrong et al. [12] and based on a phase corrective scheme. The phase mismatch in a nonlinear optical process is corrected by modulating the optical constants (electric permittivity or/and nonlinear susceptibility) of the medium with a period equal to the coherence length of the process. In our case, the fiber grating's constant is chosen to compensate for the phase mismatch between fundamental modes at different frequencies. The application of this idea for effective generation of the second harmonic has been first theoretically studied in [13], [14]. In recent works the grating-assisted generation of the second harmonic has been demonstrated experimentally in lithium niobate waveguide periodically poled by applying an external field in [15], and also in potassium niobate [16], GaAs–AlAs superlattice waveguide [17] and in silica glass fiber [18]. More recently, the QPM method has been applied to generate coherent extreme-UV light through a modulated hollow-core waveguide filled with various gases [19]. Experimental demonstration of efficient third harmonic generation in barium fluoride has been reported through self phase matching via a travelling grating induced by two non-collinear input beams [20-22]. In this configuration, the index grating leads to diffraction of the generated third harmonic.

In the present work, we detail the results of an analytical and numerical analysis which validate the grating-assisted THG concept in optical fibers. We restrict here our discussion to the case of continuous wave (CW) pumping. The paper is organized as follows: in section II we introduce theoretical formulations which allow calculating efficiency of energy conversion using nonlinear coupled mode equations and coupled generalized nonlinear Schrödinger equations (GNLSE). Section III provides illustrative example design of the step-index fiber and analysis of conversion efficiency obtained by using analytical and numerical approaches. We

(28 September 2010) All authors acknowledge bilateral French-Polish program "Polonium". W. Urbanczyk acknowledges the Statutory Grant at Wroclaw University of Technology, K. Tarnowski, acknowledges support of the Foundation for Polish Science within "MISTRZ" Programme and "Młoda kadra" – Fellowship co-financed by European Union within European Social Fund.

W. Urbanczyk, K. Tarnowski are with the Institute of Physics, Wroclaw University of Technology, Wroclaw, Poland (e-mails: waclaw.urbanczyk@pwr.wroc.pl, karol.tarnowski@pwr.wroc.pl; phone: +48 (71) 320 33 85)

B. Kibler, C. Finot are with the Laboratoire Interdisciplinaire Carnot de Bourgogne, UMR 5209 CNRS - Université de Bourgogne, Dijon, France (e-mails: bertrand.kibler@u-bourgogne.fr, christophe.finot@u-bourgogne.fr; phone +33 380 395 932).

implement gradually the linear and nonlinear effects induced by the grating in both models. Section IV contains conclusions.

II. Theoretical formulation

To analyze the process of THG in longitudinally structured medium we have applied two different approaches. First, following the considerations earlier presented for quasi-phase matched second harmonic generation by Suhara and Nishihara in [13], we have used the nonlinear coupled mode theory. For comparison, we have also derived and numerically solved a system of two coupled GNLSEs allowing for investigations of THG process.

A. *Coupled mode theory*

To derive equations describing the efficiency of the THG, we started with assumption that only two modes: pump at frequency ω and its TH at 3ω propagate in the optical fiber. To describe the fiber in terms of material constants used in coupled mode theory such as electric permittivity and nonlinear susceptibility, we applied an appropriate conversion of common parameters. The electric permittivity is calculated as square of effective refractive index and average nonlinear susceptibility $\chi^{(3)}$ is calculated from nonlinear refractive index n_2 and effective refractive index n:

$$\chi^{(3)} = \frac{4}{3}\varepsilon_0 c n^2 n_2, \tag{1}$$

where ε_0 is the vacuum permittivity, and c is a light velocity. The modulation of $\chi^{(3)}$ is introduced into the coupled mode equations to describe modulation of effective mode area, which implies modulation of overlapping coefficients in frequency mixing processes.

In coupled mode theory we treat the longitudinal modulation of refractive index (which is introduced by the fiber grating) as a small perturbation. Moreover we treat nonlinearity as a perturbation. Then the canonical modes are calculated for a fiber without nonlinearity and without longitudinal modulation of refractive index. Afterwards, taking into account the parameters of the grating such as amplitude and period, we are able to describe coupling between modes. In general, modulation of electric permittivity and nonlinear susceptibility of the grating with period Λ can be expressed with Fourier expansions:

$$\Delta\varepsilon = \sum_q \Delta\varepsilon_q \exp(-jqKz), \tag{2}$$

$$\chi^{(3)} = \sum_q \chi_q^{(3)} \exp(-jqKz), \tag{3}$$

where $K = 2\pi/\Lambda$ is the grating constant. We consider here a sinusoidal grating (see Fig. 1), which means that order q can take only the values -1, 0, 1. We also assume that $\Delta\varepsilon_q$ and $\chi_q^{(3)}$ are real. Moreover, the fiber canonical modes are calculated

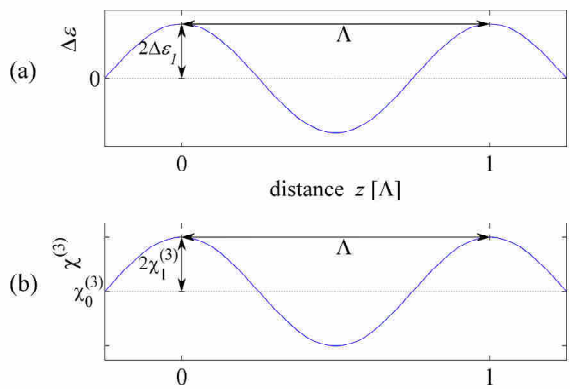

Fig. 1. (a) Modulation of relative electric permittivity $\Delta\varepsilon$ assumed in coupled mode approach. Average value of perturbation is zero, since fiber canonical modes were calculated for average ε. (b) Nonlinear susceptibility $\chi^{(3)}$ assumed in coupled mode approach. The whole nonlinearity including constant component $\chi_0^{(3)}$ is treated as perturbation.

for average electric permittivity $\langle\varepsilon\rangle_z$. In other words the zero order perturbation $\Delta\varepsilon_0$ is equal to zero and the modulation amplitude of electric permittivity is $2\Delta\varepsilon_1$ (see Fig. 1).

Starting with canonical modes, one can derive the following system of equations in the framework of coupled mode theory [23]**Erreur ! Source du renvoi introuvable.**:

$$\frac{d}{dz}A_\omega(z) = -j\frac{\omega}{4}\iint \mathbf{E}_\omega^*(x,y)\exp(+j\beta_\omega z)\mathbf{P}_\omega(x,y,z)dxdy, \tag{4}$$

$$\frac{d}{dz}A_{3\omega}(z) = -j\frac{3\omega}{4}\iint \mathbf{E}_{3\omega}^*(x,y)\exp(+j\beta_{3\omega} z)\mathbf{P}_{3\omega}(x,y,z)dxdy, \tag{5}$$

where the function $A_\omega(z)$ represents dependence of the pump amplitude upon propagation distance, $A_{3\omega}(z)$ is the amplitude of third harmonic; $\mathbf{E}_\omega(x,y)$, $\mathbf{E}_{3\omega}(x,y)$ are the normalized mode profiles of electric fields in the fundamental modes at respective frequencies.

The normalization relation is:

$$\iint \mathrm{Re}\left[\frac{1}{2}\left(\mathbf{E}_t \times \mathbf{H}_t^*\right)\right]dxdy = 1, \tag{6}$$

where subscript t denotes transverse components and **H** stands for magnetic field.

In order to solve this system of equations, one has to know the expressions for polarizations $\mathbf{P}_\omega$, $\mathbf{P}_{3\omega}$. Considering all possible frequency mixing processes, we obtain the following expressions for polarization terms oscillating with ω and 3ω.

$$\begin{aligned}\mathbf{P}_\omega &= \varepsilon_0\Delta\varepsilon_\omega\mathbf{E}_\omega + 3\varepsilon_0\chi^{(3)}_{\mathrm{SPM}\omega}(\mathbf{E}_\omega)^2\mathbf{E}_\omega^* + \\ &+ 3\varepsilon_0\chi^{(3)}_{\mathrm{THG}}\mathbf{E}_{3\omega}(\mathbf{E}_\omega^*)^2 + 6\varepsilon_0\chi^{(3)}_{\mathrm{XPM}}\mathbf{E}_{3\omega}\mathbf{E}_{3\omega}^*\mathbf{E}_\omega,\end{aligned} \tag{7}$$

$$\begin{aligned}\mathbf{P}_{3\omega} &= \varepsilon_0\Delta\varepsilon_{3\omega}\mathbf{E}_{3\omega} + \varepsilon_0\chi^{(3)}_{\mathrm{THG}}(\mathbf{E}_\omega)^3 + \\ &+ 6\varepsilon_0\chi^{(3)}_{\mathrm{XPM}}\mathbf{E}_\omega\mathbf{E}_\omega^*\mathbf{E}_{3\omega} + 3\varepsilon_0\chi^{(3)}_{\mathrm{SPM}3\omega}(\mathbf{E}_{3\omega})^2\mathbf{E}_{3\omega}^*.\end{aligned} \tag{8}$$

Using the substitutions [13]:

$$A_\omega(z) = A(z)\exp[-j(2\kappa_\omega/K)\sin(Kz)], \tag{9}$$
$$A_{3\omega}(z) = B(z)\exp[-j(2\kappa_{3\omega}/K)\sin(Kz)], \tag{10}$$

where κ_ω, $\kappa_{3\omega}$ are coupling coefficients for linear processes at both frequencies, we can write the following relations:

$$\begin{aligned}\frac{d}{dz}A = &-3j\sum_q \kappa_{\mathrm{SPM}\omega}^{(q)}\exp(-jqKz)|A|^2 A + \\ &-3j\sum_q \kappa_{\mathrm{THG}\omega}^{(q)}\exp(-j2\Delta_{-q}z)\exp(-j\varphi\sin(Kz))A^{*2}B \\ &-6j\sum_q \kappa_{\mathrm{XPM}\omega}^{(q)}\exp(-jqKz)|B|^2 A,\end{aligned} \tag{11}$$

$$\begin{aligned}\frac{d}{dz}B = &-j\sum_q \kappa_{\mathrm{THG}3\omega}^{(q)}\exp(j2\Delta_q z)\exp(j\varphi\sin(Kz))A^3 \\ &-6j\sum_q \kappa_{\mathrm{XPM}3\omega}^{(q)}\exp(-jqKz)|A|^2 B \\ &-3j\sum_q \kappa_{\mathrm{SPM}3\omega}^{(q)}\exp(-jqKz)|B|^2 B,\end{aligned} \tag{12}$$

where $\phi = 2[(\kappa_\omega - 3\kappa_{3\omega})/K]$, $2\Delta_q = \beta^{3\omega} - 3\beta^\omega - qK$ and

$$\kappa_\omega = \frac{\omega\varepsilon_0}{4}\iint|\mathbf{E}^\omega(x,y)|^2\Delta\varepsilon_\omega dxdy, \tag{13}$$

$$\kappa_{3\omega} = \frac{3\omega\varepsilon_0}{4}\iint|\mathbf{E}^{3\omega}(x,y)|^2\Delta\varepsilon_{3\omega}dxdy, \tag{14}$$

$$\kappa_{\mathrm{SPM}\omega}^{(q)} = \frac{\omega\varepsilon_0}{4}\iint|\mathbf{E}^\omega(x,y)|^4\chi_{q\mathrm{SPM}\omega}^{(3)}dxdy, \tag{15}$$

$$\kappa_{\mathrm{THG}\omega}^{(q)} = \frac{\omega\varepsilon_0}{4}\iint(\mathbf{E}^{\omega^*}(x,y))^3\mathbf{E}^{3\omega}(x,y)\chi_{q\mathrm{THG}}^{(3)}dxdy, \tag{16}$$

$$\kappa_{\mathrm{XPM}\omega}^{(q)} = \frac{\omega\varepsilon_0}{4}\iint|\mathbf{E}^\omega(x,y)|^2|\mathbf{E}^{3\omega}(x,y)|^2\chi_{q\mathrm{XPM}}^{(3)}dxdy, \tag{17}$$

$$\kappa_{\mathrm{THG}3\omega}^{(q)} = \frac{3\omega\varepsilon_0}{4}\iint\mathbf{E}^{3\omega^*}(x,y)\chi_{q\mathrm{THG}}^{(3)}\mathbf{E}^{\omega^3}(x,y)dxdy, \tag{18}$$

$$\kappa_{\mathrm{XPM}3\omega}^{(q)} = \frac{3\omega\varepsilon_0}{4}\iint|\mathbf{E}^{3\omega}(x,y)|^2\chi_{q\mathrm{XPM}}^{(3)}|\mathbf{E}^\omega(x,y)|^2 dxdy, \tag{19}$$

$$\kappa_{\mathrm{SPM}3\omega}^{(q)} = \frac{3\omega\varepsilon_0}{4}\iint|\mathbf{E}^{3\omega}(x,y)|^4\chi_{q\mathrm{SPM}3\omega}^{(3)}dxdy, \tag{20}$$

denote overlap coefficients for different nonlinear processes (THG, self phase modulation – SPM, cross phase modulation – XPM). This system of equations was then solved with MATLAB differential equation solver `ode23` to obtain the longitudinal evolution of the amplitudes of both pump and TH. The coupled mode theory can be also used to derive an approximated closed-form expression, which describes growth of TH power in initial part of process. Assuming that pump is undepleted and value of amplitude B is close to zero, the system of equations (11), (12) can be replaced with equation:

$$\frac{d}{dz}B = -j\sum_q \kappa_{\mathrm{THG}3\omega}^{(q)}\exp(j2\Delta_q z)\exp(j\varphi\sin(Kz))A^3. \tag{21}$$

After substitution of [13]:

$$\exp(j\varphi\sin(Kz)) = \sum_p J_p(\varphi)\exp(jpKz) \tag{22}$$

one can rewrite equation (21) as:

$$\frac{d}{dz}B = -j\kappa\exp(j2\Delta_q z)A^3, \tag{23}$$

where $\kappa = \kappa_{THG3\omega}^{(1)}(J_2(\varphi) + J_0(\varphi)) - \kappa_{THG3\omega}^{(0)}J_1(\varphi)$. By solving equation (21) one can obtain a simplified expression for efficiency:

$$\eta = \frac{|B|^2}{|A|^2} = \kappa^2|A|^4\left(\frac{\sin(z\Delta_q)}{z\Delta_q}\right)^2 z^2, \tag{24}$$

which gives

$$\eta = \kappa^2|A|^4 z^2 \tag{25}$$

when $\Delta_q = 0$.

This expression can be used only to estimate the conversion efficiency for short propagation distances, since important nonlinear effects as SPM and XPM were neglected in its derivation. Comparison of efficiency calculated using approximated expression with an exact solution of the equations (11-12) is presented in Fig. 3.

B. Coupled generalized nonlinear Schrödinger equations

The third harmonic generation process in longitudinally structured fiber can be also investigated using a generalized nonlinear envelope equation (GNEE) [24]. This equation has been successfully used to study non-phase-matched single-mode third harmonic generation occurring simultaneously with fs pulse spectral broadening in highly nonlinear fiber[9], [24].

The single GNEE can be expressed equivalently as a system of two coupled generalized nonlinear Schrödinger equations. This allows decreasing numerical effort by using lower number of points in frequency discretization.

In our simulations, the Raman scattering was disregarded due to its low impact on the short propagation distance studied here, while we have accounted for frequency dependence of effective mode area using approach presented in [26], [27]. Longitudinal dependence of refractive index was incorporated by solving the following equations:

$$\frac{\partial U_1}{\partial z} = \hat{D}_1(U_1) + i\frac{n_2\omega}{cA_{\text{eff}}^{1/4}} F\left\{\overline{U}_1\left(\left|\overline{U}_1\right|^2 + 2\left|\overline{U}_2\right|^2\right) + \overline{U}_1^2\overline{U}_2^*\right\}, \quad (26)$$

$$\frac{\partial U_2}{\partial z} = \hat{D}_2(U_2) + i\frac{n_2\omega}{cA_{\text{eff}}^{1/4}} F\left\{\overline{U}_2\left(\left|\overline{U}_2\right|^2 + 2\left|\overline{U}_1\right|^2\right) + \frac{1}{3}\overline{U}_1^3\right\}. \quad (27)$$

on small slices (Λ/300). In the above equations describing respectively the evolution of pump and third harmonic amplitude against propagation length [28], the following notation has been applied: $U(z,\omega)$ is the forward propagating envelope, which is normalized in such a way that $|U|^2$ yields the power in Watts; $D(z,\omega)$ is the dispersion operator in frequency domain; n_2 is the nonlinear coefficient, $A_{\text{eff}}(z,\omega)$ is the effective mode area and $\overline{U} = F^{-1}\left\{U/A_{eff}^{1/4}\right\}$, where F and F^{-1} denote respectively direct Fourier transform and inverse Fourier transform, and the subscripts 1 and 2 denote respectively pump and TH.

To ensure accurate modeling, we have verified that spectral overlapping between pump and third harmonic fields do not occur but also that higher harmonic generation is negligible. Moreover, the relevance of coupled equations system is the explicit appearance of coupling terms which allows an easier interpretation of the dynamics involved. The equations are coupled by terms representing flow of energy from pump to third harmonic - $\frac{1}{3}\overline{U}_1^3$, from third harmonic to the pump - $\overline{U}_1^2\overline{U}_2^*$ and by cross phase modulation terms.

III. Numerical Example

In this section, we present the result of simulations providing a proof of principle for grating-assisted generation of TH in optical fiber. Although the considered fiber was not optimized for maximum efficiency, the simulation results confirm the possibility of effective THG using quasi-phase-matching with refractive-index grating.

We have considered a step index fiber with germanium doped core, doping level of 7.34% and radius of 2.65 μm. This slightly different design from the standard single mode fiber (SMF28) allows here the study of higher modulation of the core index induced by the grating. We have calculated frequency dependence of effective index of the fundamental mode taking into account chromatic dispersion of pure and doped silica [29] and assumed that the fiber nonlinearity equals a constant $n_2 = 2.6\cdot10^{-20}$ m^2/W [28]. For the coupled mode approach, the average nonlinear susceptibility $\chi^{(3)}_{\text{SPM}\omega}$ and $\chi^{(3)}_{\text{SPM}3\omega}$ were calculated applying formula (1), explicitly:

$$\chi^{(3)}_{\text{SPM}\omega} = \frac{4}{3}\varepsilon_0 c n_\omega^2 n_2, \quad (28)$$

$$\chi^{(3)}_{\text{SPM}3\omega} = \frac{4}{3}\varepsilon_0 c n_{3\omega}^2 n_2, \quad (29)$$

TABLE I
Values of Parameters Applied in Calculations

Symbol	Value at pump frequency (grating variation in %)	Value at TH frequency (grating variation in %)	Unit
n_2	$2.6\cdot10^{-20}$	$2.6\cdot10^{-20}$	[m^2/W]
n	1.45031 (±0.132 %)	1.47426 (±0.167 %)	[1]
$\chi^{(3)}_{\text{SPM}}$	$1.9365\cdot10^{-22}$ (±14.96 %)	$2.0000\cdot10^{-22}$ (±2.98 %)	[m^2/V^2]
A_{eff}	31.07	14.18	[μm^2]
f_{SPM}	0.03219(±14.96 %)	0.07052 (±2.98 %)	[μm^{-2}]

where n_ω and $n_{3\omega}$ are the mode effective indices at respective frequencies. The susceptibilities $\chi^{(3)}_{\text{THG}}$ and $\chi^{(3)}_{\text{XPM}}$ were calculated as geometric average of $\chi^{(3)}_{\text{SPM}\omega}$ and $\chi^{(3)}_{\text{SPM}3\omega}$, explicitly:

$$\chi^{(3)}_{\text{THG}} = \sqrt[4]{\left(\chi^{(3)}_{\text{SPM}\omega}\right)^3 \chi^{(3)}_{\text{SPM}3\omega}}, \quad (30)$$

$$\chi^{(3)}_{\text{XPM}} = \sqrt[4]{\left(\chi^{(3)}_{\text{SPM}\omega}\right)^2 \left(\chi^{(3)}_{\text{SPM}3\omega}\right)^2}. \quad (31)$$

The values of all parameters applied in the calculations are gathered in Table I.

Knowing the parameters of the fiber, we were able to perform simulations of conversion efficiency η, which is defined as the ratio of the power in third harmonic to the initial pump power. In the simulations, we assumed that the fiber is pumped with CW laser of 10 kW power at λ = 1.5 μm. This power level is presently achievable only for pulse pumping, however we can treat CW pump as approximation of pulse pump with ns or ps pulse duration. Moreover, the stimulated Brillouin scattering nearly ceases to occur for such short pump pulses [28].

A. Fiber without grating

For the fiber without refractive index grating, the non phase matched THG process is observed with low maximal efficiency and oscillations with period equal to the coherence length calculated from the following relation:

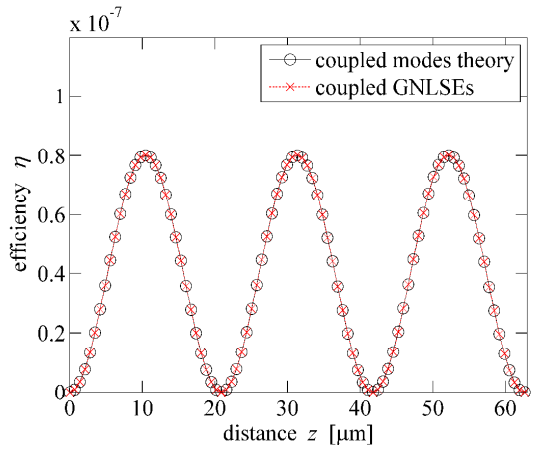

Fig. 2. Conversion efficiency η against propagation distance z in the fiber without grating calculated over 3 coherence lengths.

$$L_{\mathrm{COH}} = 2\pi/(\beta_{3\omega} - 3\beta_{\omega}) \tag{32}$$

where β stands for the propagation constant at respective frequency. As it is shown in Fig.2, the results obtained for both models are in excellent agreement.

B. Fiber with linear effects of grating

The grating inscribed in the fiber core changes its refractive index. We have calculated effective refractive index assuming that maximum increase of the core index induced by the grating fabrication is equal to 0.005. This value is achievable for germanium doped fiber with UV inscribed grating, which was hydrogen loaded before inscribing process [30]-[31].

Assuming that only effective refractive index was changed by inscribing the grating (a case of linear grating) and that grating's constant K fulfils the following quasi phase matching condition:

$$\beta_{3\omega} - 3\beta_{\omega} - K = 0, \tag{33}$$

we have obtained the efficiency of THG presented in Fig. 3. We have calculated efficiency also with approximated closed-form equation (25). As expected the initial (up to 0.5 cm of propagation distance) growth of TH is described accurately, however this expression fails to predict the maximum efficiency. We specify that small oscillations induced by the QPM technique have been averaged for better clarity in Fig. 3-7.

The maximum efficiency achieved is about 250 times greater than in the fiber without grating. The analytic and numerical models give similar results for the growth rate of TH power, however slight discrepancies appear both in the position and the maximum value of efficiency. This difference between both models is studied in details in the following. In this configuration, the achieved maximum efficiency is low and reaches only about 2×10^{-5}, because the quasi-phase matching condition represented by (33) does not take into account nonlinear change of refractive index.

Indeed, to achieve greater conversion efficiency than presented in Fig. 3, a nonlinear correction should be included in the condition (33). Since nonlinear effects change the propagation constant, we should introduce nonlinear propagation constants expressed in the following way [28]:

$$\tilde{\beta}_{\omega} = \beta_{\omega} + \frac{n_2\omega}{c} f_{\mathrm{SPM}\omega} P_{\omega} + 2\frac{n_2\omega}{c} f_{\mathrm{XPM}} P_{3\omega}, \tag{34}$$

$$\tilde{\beta}_{3\omega} = \beta_{3\omega} + \frac{n_2 3\omega}{c} f_{\mathrm{SPM}3\omega} P_{3\omega} + 2\frac{n_2 3\omega}{c} f_{\mathrm{XPM}} P_{\omega}, \tag{35}$$

where P_{ω} and $P_{3\omega}$ stand for power in pump and in its third harmonic, and the f coefficients denote overlap integrals defined in the same manner as in [28], [32]. Assuming that power in the third harmonic is low and can be neglected in the above relations, we obtain the simplified nonlinear phase

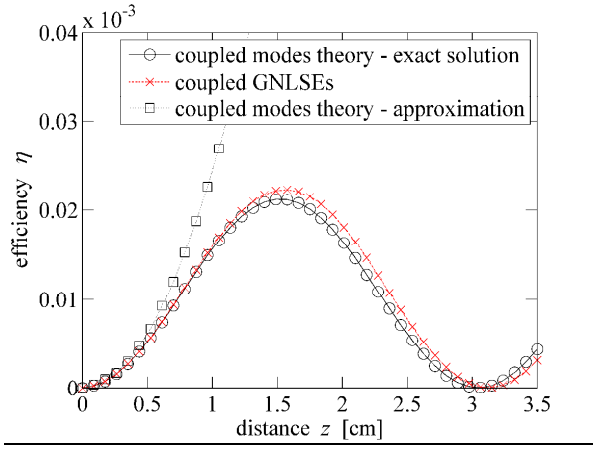

Fig. 3. Conversion efficiency η against propagation distance z in the fiber with linear refractive index grating satisfying linear phase matching condition (33)

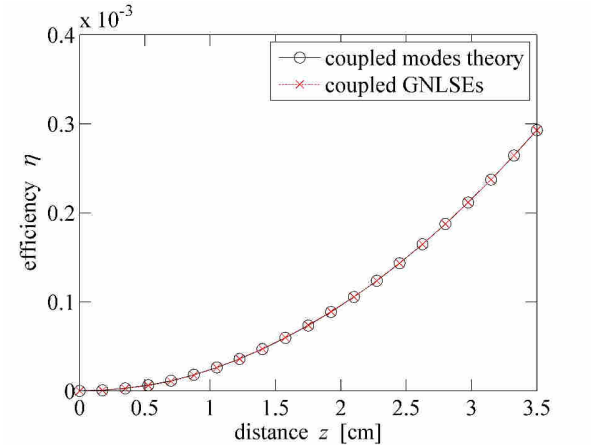

Fig. 4. Conversion efficiency η against propagation distance z in fibers with linear refractive index grating satisfying nonlinear (36) phase matching conditions.

matching condition:

$$\beta_{3\omega} - \beta_{\omega} + \frac{n_2 3\omega}{c}(2 f_{\mathrm{XPM}} - f_{\mathrm{SPM}\omega})P_{\omega} - K = 0. \tag{36}$$

In Fig. 4, we present the results of calculations obtained for the above nonlinear phase matching condition. It clearly proves that applying corrected phase matching condition results in significant increase of the conversion efficiency (more than one order of magnitude over the same distance).

C. Fiber with linear and nonlinear effects of grating

The analysis presented so far does not take into account that the change of the core refractive index has influence not only on the propagation constant but also on mode field diameter. Consequently, the grating introduces modulation of the fiber nonlinear parameters related to the mode effective area and the overlapping coefficients.

To evaluate the effect of modulation of nonlinear parameters on conversion efficiency, we have calculated the mode effective areas for extreme values of refractive index in

the grating and we have assumed that the inverse of effective mode area (i.e., the overlap coefficient $f_{\mathrm{SPM}\omega}$ or $f_{\mathrm{SPM}3\omega}$) changes sinusoidally between the extreme points (see Table I). This assumption can be incorporated in the coupled GNLSEs numerical solution by accounting for $A_{\mathrm{eff}}(z)$ dependency. It means that in the considered model the mode effective area varies both with frequency and propagation distance.

Incorporating of sinusoidal modulation of the inverse of mode effective area into the coupled modes theory is not straightforward because in this approach nonlinearity of the material is represented only by nonlinear susceptibility. Knowing the values of effective area in extremes of the grating, we have determined the relative change in the inverse of effective area (given in Table I) and introduced equivalent variation of nonlinear susceptibilities into the coupled modes approach by setting respective values of $\chi^{(3)}_{q\mathrm{SPM}\omega}$, $\chi^{(3)}_{q\mathrm{SPM}3\omega}$, $\chi^{(3)}_{q\mathrm{THG}}$, and $\chi^{(3)}_{q\mathrm{XPM}}$ for q = -1, 1.

The results presented in Fig. 5 were obtained for the linear phase matching condition (33). It appears that also accounting for modulation of nonlinearity leads to significant increase of the conversion efficiency reaching two orders of magnitude compared to the linear grating discussed in the previous section, see Fig. 3. Here, it turns out that grating induced nonlinearity modulation impacts more significantly the THG process than the linear refractive index modulation. This is simply due to higher relative modulation of the effective mode area compared to refractive index modulation as reported in Table I. The QPM technique is indeed highly sensitive to the modulation amplitude of optical constants of the medium. Similarly to the case of the linear grating both models give the same results for initial growth rate of the TH. A slight difference is still observed for the maximum conversion efficiency.

In Fig. 6, we show the results obtained taking into account nonlinearity modulation introduced by the grating and nonlinear quasi phase matching condition represented by (36).

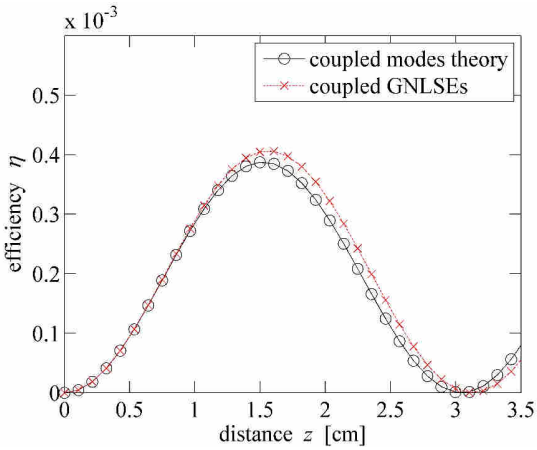

Fig. 5. Conversion efficiency η against propagation distance z in the fiber with nonlinear refractive index grating satisfying the linear phase matching condition (33).

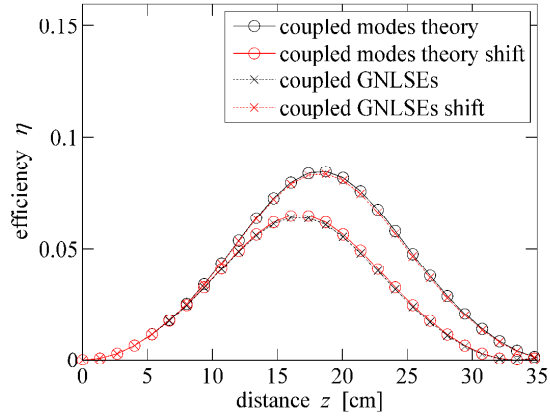

Fig. 6. Conversion efficiency η against propagation distance z in the fiber with nonlinear refractive index grating satisfying the nonlinear quasi phase matching condition (36).

Conversion efficiency in the range 5-10% over propagation distance below 20 cm is obtained. This distance corresponds to about 9000 periods of the grating. The values of maximal efficiency and its position predicted by both models are not exactly the same. This can be related to the fact that coupled mode theory does not integrate combined effects of both dispersion and nonlinearity in the same way than coupled GNLSEs. Consequently, a slight phase-mismatch seems to be cumulated during the propagation. Indeed, when the grating constant is shifted by the same small absolute value in either model we then obtained an excellent good agreement between both models, as shown in Fig. 6. The small correcting term used is equal to 5 m^{-1} (1.66×10^{-5} of the total phase mismatch).

D. *Optimization and discussion*

Previously we assumed that TH power can be neglected in the relation defining the grating period. A more rigorous study would take into account the impact of both pump depletion and TH amplification during propagation on the relation (36), this leads to investigate longitudinal variations of the grating period and then considers more complex chirped gratings. However, one may ask if better efficiency can be simply reached by adding a small shift ζ in the phase matching condition corresponding to the third harmonic contribution:

$$\beta_{3\omega} - 3\beta_{\omega} + \frac{n_2 3\omega}{c}(2f_{\mathrm{XPM}} - f_{\mathrm{SPM}})P_{\omega} + \varsigma - K = 0. \qquad (37)$$

We have performed numerical optimization of TH conversion based on this last phase matching condition by using the coupled modes theory (see Fig. 7). Finally we have found that a maximum conversion about 20% is obtained for ζ = -23 m^{-1} over 45 cm of propagation. This optimization value corresponds to about 10-20% of the nonlinear contribution induced by the pump power in the relation (37), which is of the same order than the conversion efficiency, thus confirming the influence of TH power. These results have also been confirmed by the coupled GNLSEs model.

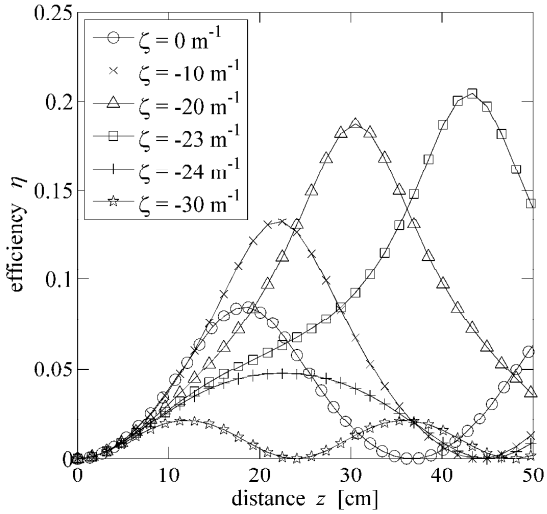

Fig. 7. Conversion efficiency η against propagation distance z in the fiber with nonlinear refractive index grating satisfying the nonlinear quasi phase matching condition (37).

These last results highlight the high sensitivity of the THG process to slight phase shifts in this configuration. This effect is mainly due to the narrow bandwidth allowed by the QPM technique based on constant grating period. Such a constraint could be relaxed by using chirped gratings which simultaneously enable very high efficiency with broadened phase matching bandwidth [13].

IV. Conclusion

We analyzed efficiency of energy conversion from pump to its third harmonic in conventional step index fiber based on grating-assisted quasi-phase matching technique. For this purpose, we developed analytical formulation in the framework of coupled mode theory, which allows accounting for modulation of both linear and nonlinear parameters of the fiber with longitudinal modulation of refractive index in the core. For comparison, we also used a fully numerical model employing coupled GNLSEs. In both approaches we have used continuous wave pumping. The results predicted by both models are in good agreement.

Our simulation results show that the grating must satisfy the nonlinear quasi-phase matching conditions represented by (36), (37) in order to reach maximum efficiency. Moreover, including in the simulation a modulation of the grating nonlinear parameters leads to significant increase of the conversion efficiency. For the optimum period of the nonlinear grating, the efficiency reaching 20% over the propagation distance of 45 cm can be achieved, whereas in fiber without grating the maximum efficiency is only 10^{-7}. A possible way of further improvement of the efficiency could be application of microstructured fiber owing to its small mode area and high nonlinearity. Moreover, increase of efficiency is expected by application of high power femtosecond pump pulses, however in this case a special fiber design matching the group velocity at pump and TH frequencies is necessary to avoid the effect of pulse walk-off.

In this paper we have focused only on grating-assisted THG process as a possible solution of the phase mismatch problem encountered in conventional fibers. It is worth to mention that similar approach can be also applied to enhance other processes of wavelength conversion like four wave mixing and supercontinuum generation.

References

[1] J. M. Gabriagues, "Third-harmonic and three-wave sum-frequency light generation in an elliptical-core optical fiber," *Optics Letters*, vol. 8, no. 3, pp. 183-185, Mar. 1983

[2] D. L. Nicácio, E. A. Gouveia, N. M. Borges, A. S. Gouveia-Neto, "Third-harmonic generation in GeO_2-doped silica single-mode optical fibers," *Applied Physics Letters*, vol. 62, no. 18, pp. 2179-2181, May 1993

[3] J. Thøgersen, J. Mark, "Third harmonic generation in standard and erbium-doped fibers," *Optics Communications*, vol. 110, no. 3-4, pp. 435-444, Aug. 1994

[4] I. A. Bufetov, M. V. Grekov, K. M. Golant, E. M. Dianov, R. R. Khrapko, "Ultraviolet-light generation in nitrogen-doped silica fiber," *Optics Letters*, vol. 22, no. 18, pp. 1394-1396, Sep. 1997

[5] A. Efimov, et al., "Phase-matched third harmonic generation in microstructured fibers," *Optics Express*, vol. 11, no. 20, pp. 2567–2576, Oct. 2003

[6] E. E. Serebryannikov et al., "Third-harmonic generation by Raman-shifted solitons in a photonic-crystal fiber," *Journal of the Optical Society of America B*, vol. 23, no. 9, pp. 1975-1980, Sep. 2006

[7] F. G. Omenetto et al., "Polarization dependent harmonic generation in microstructured fibers," *Optics Express*, vol. 11, no. 1, pp. 61–67, Jan. 2003

[8] V. Grubsky, A. Savchenko, "Glass micro-fibers for efficient third harmonic generation," *Optics Express,* vol. 13, no. 18, pp. 6798–6806, Sep. 2005

[9] B. Kibler, R. Fischer, G. Genty, D. N. Neshev, J. M. Dudley, "Simultaneous fs pulse spectral broadening and third harmonic generation in highly nonlinear fiber: experiments and simulations," *Applied Physics B*, vol. 91, pp. 349-352, May 2008

[10] G. Qin et al., "Second and third harmonics and flattened supercontinuum generation in tellurite microstructured fibers," *Optics Letters*, vol. 35 no. 1, pp 58–60, Jan. 2010

[11] A. Bétourné, Y. Quiquempois, G. Bouwmans, M. Douay, "Design of a photonic crystal fiber for phase matched frequency doubling or tripling," *Optics Express*, vol. 16, no. 18, pp. 14255-14262, Sep. 2008

[12] J. A. Armstrong, N. Bloembergen, J. Ducuing, P. S. Pershan, "Interactions between light waves in a nonlinear dielectric," *Physical Review,* vol. 127, no. 6, pp. 1918-1939, Sep. 1962

[13] T. Suhara, H. Nishihara, "Theoretical Analysis of Waveguide Second-Harmonic Generation Phase Matched with Uniform and Chirped Gratings," *IEEE Journal of Quantum Electronics,* vol. 26, no. 7, pp. 1265-1276, Jul. 1990

[14] M. M. Fejer, G. A. Magel, D. H. Jundt, R. L. Byer, "Quasi-Phase-Matched Second Harmonic Generation: Tuning and Tolerances," *IEEE Journal of Quantum Electronics,* vol. 28, no. 11, pp. 2631-2654, Nov. 1992

[15] M. Yamada, N. Nada, M. Saitoh, K. Watanabe, "First-order quasi-phase matched $LiNbO_3$ waveguide periodically poled by applying an external field for efficient blue second-harmonic generation," *Applied Physics Letters*, vol. 62, no. 5, pp. 435-436, Feb. 1993

[16] J.-P. Meyn, M. E. Klein, D. Woll, R. Wallenstein, "Periodically poled potassium niobate for second-harmonic generation at 463 nm," *Optics Letters,* vol. 24, no. 16, pp. 1154-1156, Aug. 1999

[17] A. Saher Helmy et al., "Quasi phase matching in GaAs–AlAs superlattice waveguides through bandgap tuning by use of quantum-well intermixing," *Optics Letters*, vol. 25, no. 18, pp. 1370–1372, Sep. 2000

[18] T. Mizunami, Y. Sadakane, Y. Tatsumoto, "Second-harmonic generation from thermally-poled twin-hole silica-glass optical fiber and

enhancement by quasi phase matching," *Thin Solid Films*, vol. 516, no. 17, pp. 5890–5893, Jul. 2008

[19] A. Paul et al., "Quasi-phase-matched generation of coherent extreme-ultraviolet light," *Nature,* vol. 421, pp. 51-54, Jan. 2003

[20] Th. Schneider, R. P. Schmid, J. Reif, "Efficient self phase matched third harmonic generation of ultrashort pulses in a material with positive dispersion," *Applied Physics B,* vol. 72, pp. 563-565, Feb. 2001

[21] Th. Schneider, J. Reif, "Influence of an ultrafast transient refractive-index grating on nonlinear optical phenomena," *Physical Review A,* vol. 65, pp. 023801, Jan. 2002

[22] J. Reif, R. P. Schmid, Th. Schneider, "Femtosecond third-harmonic generation: self-phase matching through a transient Kerr grating and the way to ultrafast computing," *Applied Physics B,* vol. 74, pp. 745-748, Jun. 2002

[23] H. Nishihara, M. Haruna, and T. Suhara, *Optical Integrated Circuits*, New York, McGraw-Hill, 1989, pp. 46-61

[24] G. Genty, P. Kinsler, B. Kibler, J. M. Dudley, "Nonlinear envelope equation modeling of sub-cycle dynamics and harmonic generation in nonlinear waveguides," *Optics Express*, vol. 15, no. 9, pp. 5382–5387, Apr. 2007

[25] G. Genty, B. Kibler, P. Kinsler, J. M. Dudley, "Harmonic extended supercontinuum generation and carrier envelope phase dependent spectral broadening in silica nanowires," *Optics Express*, vol. 16, no. 15, pp. 16886- 16893, Jul. 2008

[26] J. Lægsgaard, Mode profile dispersion in the generalized nonlinear Schrödinger equation," *Optics Express*, vol. 15, no. 24, pp. 16110–16123, Nov. 2007

[27] J. M. Dudley, J. R. Taylor, *Supercontinuum Generation in Optical Fibres,* Cambridge, Cambridge University Press, 2010, pp. 32-51.

[28] G. P. Agrawal, *Nonlinear Fiber Optics*, 4th ed., New York, Academic Press, 2007

[29] R. B. Dyott, *Elliptical Fiber Waveguides*, Norwood, Artech House, 1995, pp. 100-102

[30] P. J. Lemaire, R. M. Atkins, V. Mizrahi, W. A. Reed, "High pressure H_2 loading as a technique for achieving ultrahigh UV photosensitivity and thermal sensitivity in GeO_2 doped optical fibers," *Electronics Letters*, vol. 29 no. 13, pp 1191–1193, Jun. 1993

[31] S. A. Vasil'ev et al., "Fibre gratings and their applications," *Quantum Electronics*, vol. 35, no. 12, pp. 1085–1103, Dec. 2005

[32] R. H. Stolen, J. E. Bjorkholm, "Parametric Amplification and Frequency Conversion in Optical Fibres," *IEEE Journal of Quantum Electronics*, vol. QE-18, no. 7, pp. 1062-1072, Jul. 1982